Journal of Polymers and the Environment (2020) 28:962–972
https://doi.org/10.1007/s10924-020-01657-3

ORIGINAL PAPER

Catalytic Application of Silver Nanoparticles in Chitosan Hydrogel Prepared by a Facile Method

Mohammad Sherjeel Javed Khan[1,2] · Sher Bahadar Khan[1,2] · Tahseen Kamal[1,2] · Abdullah M. Asiri[1,2]

Published online: 24 January 2020
© Springer Science+Business Media, LLC, part of Springer Nature 2020

Abstract
In this research work, a simple method of silver nanoparticles' self-synthesis in chitosan (CH) biopolymer hydrogels without utilizing a reducing agent is shown. The synthesized material was used as a catalyst in different reduction reactions. For this purpose, different amounts of CH powder were dissolved in acidic aqueous solutions and then crosslinked it with the formaldehyde solution to make a CH biopolymer hydrogel. Among all the prepared samples, a CH hydrogel prepared from a dense solution was found to be suitable for this study because of good mechanical stability. For the self-synthesis of silver nanoparticles inside hydrogel, it was immersed in an aqueous solution of $AgNO_3$ (10 mM) for 3 days at room temperature. The color of the chitosan hydrogel changed to brown from transparent which indicated the successful formation of silver nanoparticles on CH hydrogel (Ag-CH). No reducing agent for conversion of the Ag^{1+} ions to nanoparticles in this whole synthesis method. Instrumental techniques such as FESEM, XRD and EDX analysis confirmed the successful preparation of Ag-CH. The Ag-CH was checked as a catalyst in the 2-nitrophenol (2-NP) and acridine orange (ArO) reduction reactions. Both reactions were carried out at high rate constants (2-NP = 0.260 min^{-1}, ArO = 0.253 min^{-1}) by using the Ag-CH hydrogel catalyst. In addition, we discussed the mechanism of action of the reducing agent, the effect of k_{app} on the two reduction reactions of Ag-CH and the recyclability.

Keywords Chitosan · Hydrogel · Silver nanoparticles · Acridine orange · 2-Nitrophenol

Introduction

With the rapid development of industrialization, a considerable amount of waste is continuously discharged into the environment through nearby water streams. Although clean water is important to society, these ongoing waste treatment processes tend to reduce the quality of water [1–3]. In particular, organic compounds such as dyes can contaminate the aqueous environment if not properly processed by textiles, paint, food, leather and paper industries [4–7]. Synthetic dyes have a wide range of uses which makes their use unavoidable. The only way to handle these dye contaminants is to develop safe disposal mechanisms and methods so that they can coexist with the ecosystem to provide a friendly environment. Until now, many wastewater treatment strategies, such as neutralizing acidic and alkaline fluids, chemical oxidation and flocculation, effluents containing activated carbon and added organic carbon, biodegradable tools and catalytic techniques have been explored [8–17]. Among the above-mentioned strategies, catalysis is considered to be most suitable because it is energy-sustainable, environmentally compatible, and results in the complete or partial degradation of dye contaminants. In particular, various types of dyes have been used to simulate organic contaminants in wastewater [18].

Removal of different toxic chemicals such as azo dyes, heavy metal ions, pesticides and pollutants from wastewater can be achieved by various techniques. Mainly, chemical and physicochemical methods are involved in the said purpose [19]. Sometimes combination of the methods like adsorption, biological systems, chemical precipitation, membrane processes, reverse osmosis, ion-exchange, ultrafiltration are used. The choice of solvent extraction combined with

✉ Tahseen Kamal
tkkhan@kau.edu.sa

✉ Abdullah M. Asiri
aasiri2@kau.edu.sa

[1] Department of Chemistry, Faculty of Science, King Abdulaziz University, Jeddah, Saudi Arabia

[2] Center of Excellence for Advanced Materials Research, King Abdulaziz University, Jeddah, Saudi Arabia

different methods depends on the concentration of contaminants in the wastewater [20].

Nitrophenol (NP) is a common organic compound with a variety of industrial applications in the pharmaceutical, explosive, dye and agrochemical industries. Most NPs possess toxicity to human health. Among such nitrophenols, the substituted nitro groups containing such as 4-nitrophenol (4-NP), 2,4-dinitrophenol, 2-nitrophenol and the like are present. US Environmental Protection Agency considers NPs as the most toxic contaminant. It is because its short-term inhalation can lead to serious health issues such as headache, vomiting, purpura and lethargy [21–23]. Therefore, due to these facts about various NPs, scientists are now looking for appropriate method for removing them from aqueous bodies or converting it to less-toxic chemicals. In this regard, the reduction of NPs by a suitable catalyst with the use of reducing agent in an aqueous medium to produce aminophenols (APs) is a facile process of dealing these toxic compounds [24, 25]. In fact, other methods could be used for such compounds removal from water bodies but catalytic reduction is one of the most effective, environmentally friendly and low cost method. This process is also suitable and acceptable for large scale industries. Over the past two decades, numerous metal and metal oxide nanoparticles-based catalysts like copper, palladium, silver, gold and platinum etc. have been tested as catalysts for the said reduction reactions. It was found that the catalytic activity of catalysts mostly depends on the size, shape and nature of the nanoparticles [26–29]. The decrease in the catalytic activities were observed due to the nanoparticle's aggregation. Aggregation of nanoparticles occur easily, and its prevention is utmost important. These agglomerated nanoparticles lead to a reduction in the surface area, thus lowering the catalytic activity.

So far, different metal nanoparticles have been tested as catalysts. Among such metals, silver nanoparticles (AgNP) have attracted a great deal of attention due to their cost-performance ratio with other noble metals [30, 31]. To help prevent the metal nanoparticles from aggregation, the use of solid polymeric supports is a commonly adopted method. Polymers in different forms such as microfibers [32–34], nanofibers [35–37], sheets [38], films, and spheres [39–41], hydrogels and other forms [42, 43]have been used as catalytic supports. All such studies necessarily used the reducing agents like sodium borohydride, citric acid or hydrazine for the synthesis of metal nanoparticles. However, the easy green synthesis of AgNP with high catalytic activity remains an important challenge [44, 45].

Chitosan (CH) is a deacetylated product of the second most abundantly available polymer in nature. Usually, 50% or above degree of deacetylated chitin becomes soluble in acidic aqueous medium and is referred to as CH. The dissolution of the CH in acidic medium occurs by protonation of the $–NH_2$ functional group at the C-2 position of the D-glucosamine repeating unit. As a result, the CH polysaccharide converts to a polyelectrolyte. Due to its abundantly availability in nature, it finds many subsequent uses. CH has been used in many studies due to its biocompatible and easy availability from cheap sources. It is usually processed in the form of its acidic aqueous solution to form variety of desirable products such as nanofibers, coatings, hydrogels and films.

Owing to the low cytotoxicity and enzymatic degradation, hydrogels consisting of CH and other polysaccharides are widely used as the main material in a variety of biomedical applications such as tissue engineering, therapeutic drug delivery and medical implants [46, 47]. Recently, we used it as a coating material for enhanced immobilization of the metal nanoparticles over microscopic substrates which were used as dip catalysts for the reduction of the toxic organic pollutants[32–34, 48]. From these studies, it was found as an excellent coating material. Previously, many synthetic polymer-based hydrogels such as *p*(methacrylic acid-*co*-acrylonitrile)-metal (metal: Co and Cu) microgel [49], poly(*N*-isopropylacrylamide-*co*-allylacetic acid) microgels [50], cationic microgels embedding metal nanoparticles [51] and cobalt loaded poly(2-acrylamido-2-methyl-1-propansulfonic acid) hydrogels [52] have been used for the immobilization of catalytic metal nanoparticles.

In contrast to synthetic polymer-based hydrogels, we chose to use the CH hydrogel for the synthesis of the AgNp and their use as a catalyst for catalyzing the water-based reduction processes of toxic organic compounds.

Experimental

Materials

Yellowish powder high molecular weight chitosan with a degree of deacetylation of 75% was bought from Sigma-Aldrich, Ireland. Silver nitrate ($AgNO_3$, 169.87 g/ml) was purchased from MERCK. A reducing agent of sodium borohydride ($NaBH_4$, 37.83 g/mol) in powder form was purchased from Loba-chemie. Acetic acid (CH_3COOH, 60.05 g/mol), 2-nitrophenol ($C_6H_5NO_3$, 139.11 g/mol), acridine orange ($C_{17}H_{19}N_3$, 265.36 g/mol) and a cross linking material formaldehyde solution 38% w/w (HCHO, 30.03 g/mol) were purchased from BDH chemicals, Poole, England. All the solutions were prepared in de-ionized (DI) water.

Synthesis of Catalyst

Three different concentration solutions of CH were used for the preparation of hydrogels. 2.4 g of CH was dissolved in deionized water (30 ml containing 20% v/v acetic acid) to obtain a clear yellowish solution. A solution of formaldehyde

(4 ml) was then mixed with the CH solution by stirring for 1 h. The whole CH solution was poured into few plastic tubes. These tubes filled with polymer solution were statically kept for 24 h to transform into hydrogel. After 24 h of inspection, the CH solution solidified into a clear cylindrical hydrogel inside tubes. The CH hydrogel was obtained from the tubes and washed with NaOH solution and deionized water several times and stored.

Preparation of Ag Nanoparticles in Chitosan Hydrogel (Ag-CH)

Small pieces of the CH hydrogel were obtained by cutting the cylindrical stored hydrogels. Then known amount of CH hydrogel was added to a beaker containing an aqueous $AgNO_3$ solution (10 mM, 30 ml). The contents of the beaker were continuously stirred for 24 h. The next day, the clear CH hydrogel turned its color to slightly brown. Further, the CH hydrogel pieces were kept in the $AgNO_3$ aqueous solution for additional 48 h. After this time span, a dark brown CH hydrogel was found at the end of three days. The change in color from clear to brown in the hydrogel indicated the self-synthesis of Ag nanoparticles by crosslinked CH chains. The sample was named as Ag-CH.

Study of Catalytic Activity

The synthesized Ag-CH pieces were tested as catalyst in the reduction reaction of 2-nitrophenol (2-NP) and acridine orange (ArO) two model compounds. $NaBH_4$ was used as a reducing agent for the reduction. In a typical reduction reaction experiment of 2-NP, a clean beaker was charged with 30 ml. Thereafter, an addition of predetermined amount of Ag-CH was performed to beaker to start the stirring process. A pre-measured $NaBH_4$ amount was inserted to the stirred solution of 2-NP mixed with Ag-CH. After addition of the reducing agent, a solution (3 ml) from beaker was taken with a sterile syringe. It was then put into a quartz cuvette for measuring the UV-visible spectra with a spectrophotometer. After the spectral measurement, the solution in the cuvette is again placed in the reaction medium. The recording of the spectra was resumed until the solution in beaker became clear. The reduction reaction of ArO dye was performed in accordance with the above method. The reuse test was carried out in a similar manner except that the recovered Ag-CH was from one reaction was again used for the next batch of reactions.

Characterization

In this study, CH and Ag-CH samples were morphologically analyzed by field emission electron microscopy (FESEM). Pure CH and Ag-CH hydrogel samples were lyophilized for FESEM analysis. Lyophilized samples were coated with platinum (Pt) using a coater for 30 s prior to morphological study. X-ray diffraction study was performed using an ARL X'tra, Thermo Scientific diffractometer. The device was operated at high voltage and high current. This device is equipped with a Cu anode that generates CuK-alpha radiation (0.1542 nm). Spectroscopic data for catalytic experiments were recorded using an ultraviolet-visible spectrophotometer from Evolution 300 from Thermo Scientific.

Result and Discussion

Observation During Samples' Preparation

The preparation of CH and Ag-CH hydrogels is shown stepwise in Scheme 1. The formaldehyde solution was added to chitosan which was dissolved in acidic media. After mixing of the two solutions, it was filled into different plastic tubes and kept at static conditions for 24 h at room temperature. After 24 h, the solutions turned into hydrogels in the tubes. The tubes were broken and pure CH cylindrical hydrogels were obtained. These hydrogels were cut into pieces, neutralized with NaOH solution and further washed with DI water for removing the excess and unreacted formaldehyde, CH chains and other ions. Thereafter, the washed CH hydrogel pieces were added to an aqueous $AgNO_3$ (10 mM) solution and kept for stirring. A visual confirmation of the successful synthesis of the Ag nanoparticles inside CH hydrogel was observed by the color change.

XRD

In Fig. 1, the XRD patterns of CH and Ag-CH hydrogel are shown. The XRD pattern of CH had similar features as reported earlier. There was a single broad peak in the XRD pattern of CH hydrogel sample in the 2θ range of 20°–43°. This broad peak was due to the amorphous structure of chitosan. On the other hand, the XRD pattern of Ag-CH contains four additional peaks to the amorphous CH peak. These four peaks were due the reflections of (111), (200), (220) and (311) from a face-centered cubic unit cell of Ag metal in the range of 2θ = 35°–80° [32, 38]. The two reflections of Ag nanoparticles (111) and (220) overlapped with the amorphous peak of CH in the Ag-CH sample. Thus XRD clearly indicated the successful formation of the Ag nanoparticles inside the CH hydrogel. The Ag nanoparticles' size was determined from (111) reflection in the XRD pattern of Ag-CH sample. This peak was separated from the pattern by deconvolution and using the Scherrer's equation of $D = \frac{0.9\lambda}{\beta cos\theta}$, (where D, λ, β and θ represent the size, X-ray wavelength, peak breadth and diffraction angle, respectively)

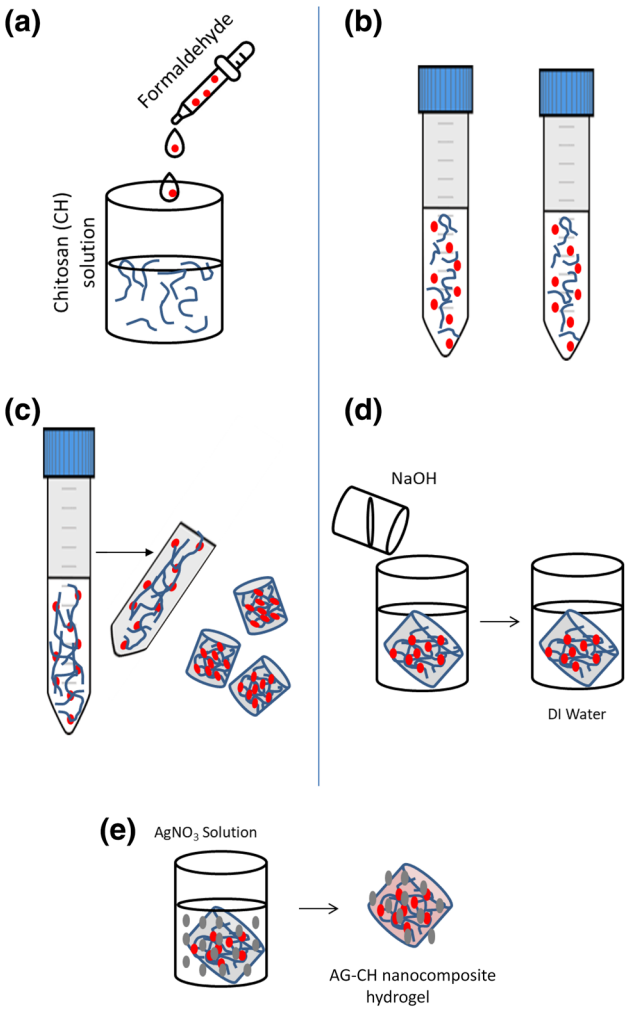

Scheme 1 Illustration of the preparation process of Ag-CH hydrogel. **a** Mixing of chitosan and formaldehyde solutions, **b** mixed solution in plastic tube as static condition for 24 h, **c** separation of hydrogel and cutting into pieces, **d** CH hydrogel washing and **e** its insertion into an aqueous $AgNO_3$ solution for the adsorption of silver ions and their in-situ reduction to the Ag nanoparticles.

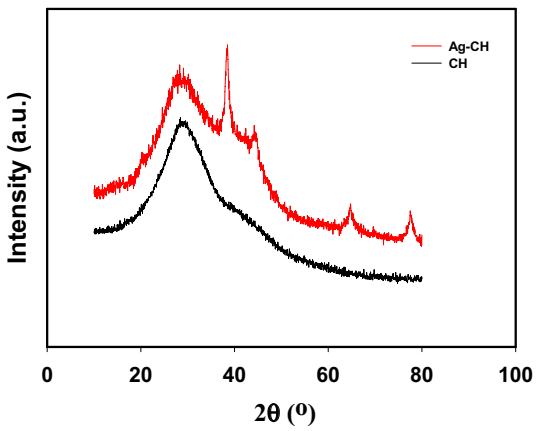

Fig. 1 XRD patterns of the freeze-dried pure CH and Ag-CH hydrogels

the size of the nanoparticles was determined. The size was estimated to be 11 nm.

FESEM

Figure 2 a shows a FESEM image of a pure CH hydrogel. The sample was made from a 8 wt/wt% CH hydrogel. It displays the hydrogel porous morphology [53, 54]. The elongated pores can be clearly observed in the surface of the sample which might be due to the collapsing of the pores while cutting the sample by knife for the morphological analysis. The existence of such pores may help in the solvent (aqueous medium) penetration to the inner of the CH hydrogel. Based-on the observed porosity, it might appear a good catalytic support. Figure 2b shows a highly enlarged image of the CH hydrogel which shows a smooth surface morphology. Moreover, no particles were observed in this image which proves that sample was pure. Figure 2c shows a highly magnified SEM image of Ag-CH. Many bright spots can be easily viewed in the surface of this sample alongwith number of cracks. It can be said that these bright spots represent the existence of Ag nanoparticles in the Ag-CH sample. The nanoparticles' sizes are in the range of 70 ± 22 nm. The larger size of the particles in FESEM as compared to the XRD results might be due to their aggregation in the hydrogel sample.

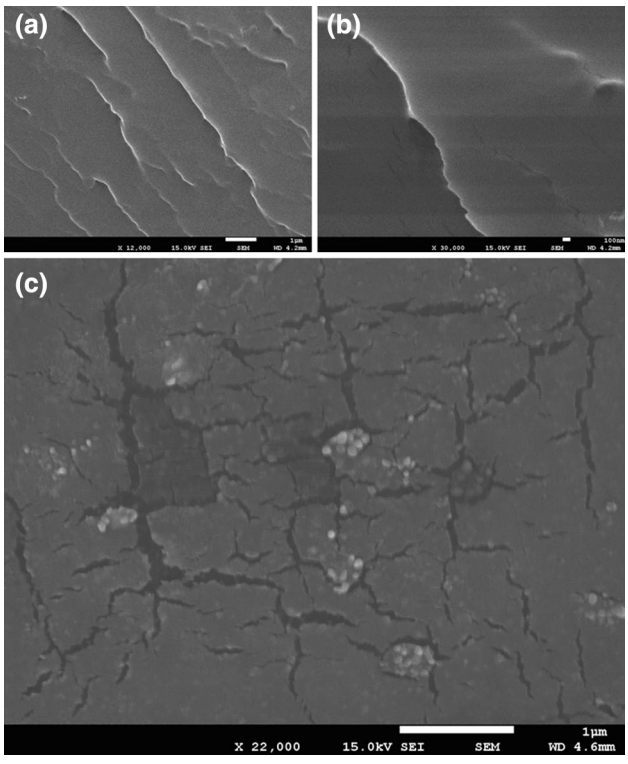

Fig. 2 FESEM images of **a** CH, **b** enlarged image of CH and **c** Ag-CH hydrogels

EDS

EDS is a reliable technique that quickly determine the elements presents in the sample. Figures 3a represents the EDS spectrum of pure CH hydrogel sample. The EDS spectrum of CH showed peaks from the four elements. These elements were nitrogen, oxygen, carbon, and platinum. The nitrogen, oxygen and carbon elements make the chitosan polymer chains while the peak of platinum element was observed due to its coating on the sample. Figure 3b shows the EDS spectrum of Ag-CH hydrogel. In this spectrum total five elements' peaks were observed which were carbon, nitrogen, oxygen, platinum and silver. The appearance of the silver peak in the EDS spectrum demonstrate the existence of the Ag nanoparticles in the Ag-CH sample.

Catalytic Investigation

The formation of amino derivatives by the reduction of corresponding aromatic nitro compounds is an industrially important process. However, $NaBH_4$, even though a strong reducing agent, cannot easily reduce the aromatic nitro compounds in aqueous or non-aqueous solution. There are many reports on the catalysis of transition metal complexes by borohydrides for the reduction of nitroaromatics [55]. The catalytic activity of Ag-CH hydrogel nanocomposites was investigated for the reduction process of 2-nitrophenol (2-NP) to 2-aminophenol (2-AP) by excess $NaBH_4$. According to some previous reports, a strong absorption peak at 277 nm is normally observed from the neutral or acidic pH solution of the 2-NP in the UV–Vis absorption spectrum [48, 56]. When $NaBH_4$ solution is added to 2-NP, the absorption peaks of 2-NP are significantly and instantly red shifted to 414 nm, corresponding to the creation of nitrophenolate ions [48]. As a result of addition of $NaBH_4$ to the 2-NP solution, a turning of the initial light yellow color of the solution to darker yellow was observed. We had similar observation during the addition of the $NaBH_4$ to the 2-NP solution. Even if an excessive amount of freshly prepared $NaBH_4$ was added to the nitrophenol solution, the intensity of the absorption peak did not significantly change for a long time, indicating that $NaBH_4$ itself cannot reduce the 2-NP molecules [57].

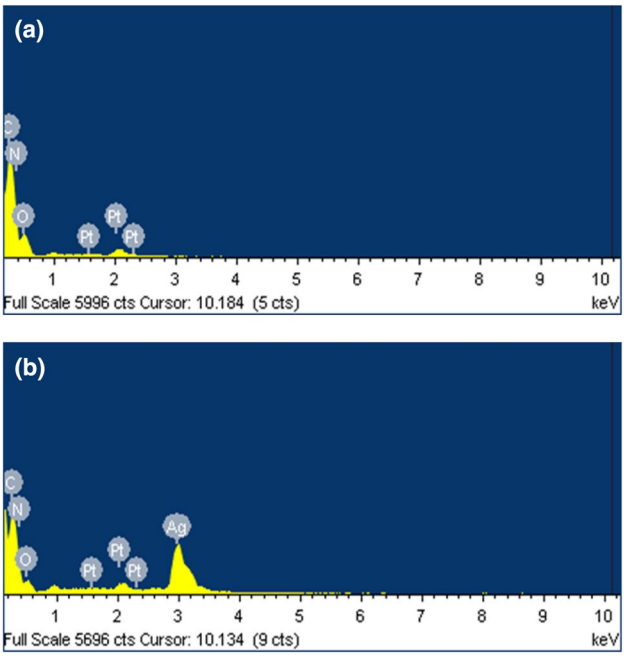

Fig. 3 Elemental analysis of the samples: EDS spectra of **a** pure CH and **b** Ag-CH hydrogels

The kinetic study of the model experiment was studied by using *pseudo-first-order* kinetic equation affected by 2-NP concentration. It is considered because the amount of $NaBH_4$ used is greater than 2-NP, and its concentration remains intact during the reduction reaction. Therefore, the rate of reduction reaction of 2-NP to 2-AP is independent of the concentration of the reducing agent. The reaction rate constant (k_{app}) is generally used to obtain the catalytic reduction property of the prepared catalyst, and the calculation method is as follows:

$$Ln\frac{C_t}{C_0} = Ln\frac{A_t}{A_0} = -k_{app}t \quad (1)$$

wherein C_0 represents the concentration of the catalyst-free nitrophenol, and C_t represents the concentration of the t reaction time (s) after the addition of the Ag-CH hydrogel and the k_{app} apparent reaction rate constant (s^{-1}).

Figure 4a indicates the uv-visible absorption spectra from the 2-NP solution. This solution had an excess amount of the $NaBH_4$, so that the conditions were feasible for the pseudo-first order kinetic reaction described above. It is distinct from this figure that the reaction of the 2-NP to 2-AP successfully progressed by the addition of the Ag-CH hydrogel catalyst because the peak intensity significantly decreased with time until it completely vanished. Figure 4b indicates the relationship between the $\ln(C_t/C_0)$ and the reaction time for 2-NP transformation to 2-AP. Moreover, additional data of the $\ln(C_t/C_0)$ and the reaction time for the reactions of the 2-NP- to 2-AP while varying the Ag-CH hydrogel catalyst is also alongside plotted in Fig. 4b. A distinct linear relationship between $\ln(C_t/C_0)$ and the reaction time for all the three reactions could be easily observed in this figure, which means that the catalytic reaction followed the *pseudo-first-order* rate law. For 2-NP, the reaction rate constants, k_{app}, calculated from the slopes of the lines were 0.260, 0.801 and 0.161 min^{-1}. Figure 4c represents the concentration ratio (%) vs reaction time. It is clear from Fig. 4c that the high quantity of the Ag-CH hydrogel catalyst resulted in the quick decolorization of the 2-NP solution as the concentration

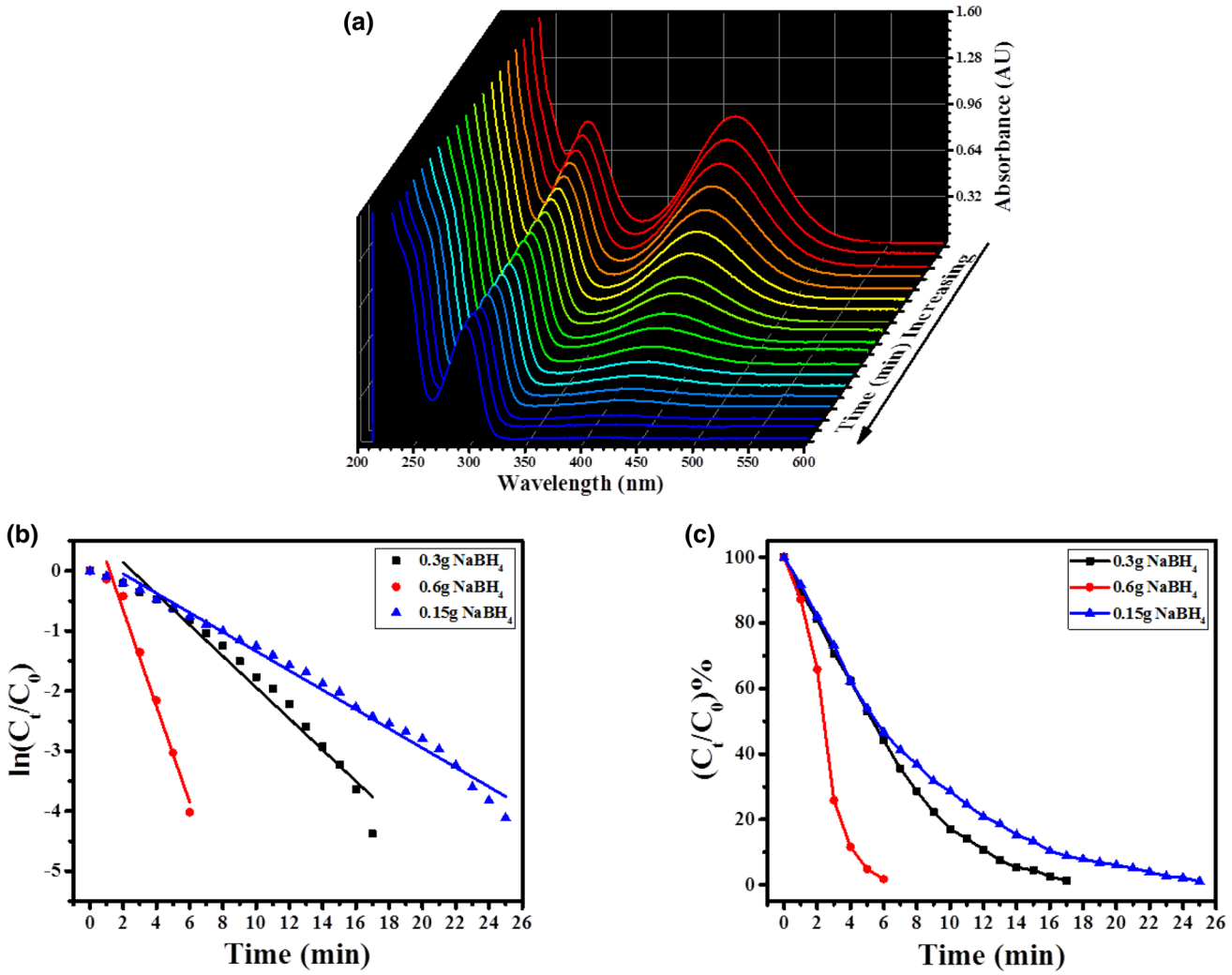

Fig. 4 The reduction reaction of 2-NP by $NaBH_4$ using Ag-CH catalyst: **a** time-dependent UV–Visible spectra of the 2-NP solution in the course of reaction, **b** $\ln(C_t/C_0)$ vs time plot while testing the different amounts of $NaBH_4$, and **c** plot of C_t/C_0 (%) vs time

ratio quickly decreased over time. Similarly, the use of lowest quantity of the Ag-CH hydrogel catalyst took longer time to decolorize the 2-NP solution. Such results are in correlation with the literature reports[36, 56, 58].

Acridine orange is broadly recognized and used in a variety of fields, including assessment of sperm chromatin quality and epifluorescence microscopy. Its staining is mainly beneficial for quick screening of ordinarily sterile specimens. It is advised for use the detection of microorganisms in direct smears prepared from different materials in fluorescence microscopy. ArO is a versatile fluorescent dye used to stain the acid vacuoles (autophagosomes, lysosomes and endosomes), DNA and RNA of living cells. It irritates the mucous membranes and the upper respiratory tract. Inhalation, ingestion or skin absorption may be harmful. The substance may irritate the eyes, skin or respiratory system. Its widespread use causes problems for the environment and humans, so it must be removed. In addition to many other ways of dealing with the pollutants in water, the catalytic reduction is now-a-days considered best to reduce the toxicity. Figure 5a represents the UV–Visible spectra recorded from ArO aqueous solution during its $NaBH_4$ reduction process. In this reaction, 0.1 g of Ag-CH hydrogel was used as a catalyst. After the 0.3 g of $NaBH_4$ and catalyst (Ag-CH) were combined to the ArO solution, the absorption intensity at $\lambda_{max} = 265$ and 466 nm began to decrease as the time passed. Such results indicate that $NaBH_4$ alone was unable to well reduce the dye molecules of ArO in the aqueous form. Based-on the spectral results from the ArO dye aqueous solution, the complete reduction of ArO was achieved in the time span of 8 min as the absorption intensity at 466 nm completely disappeared. Furthermore, the UV-visible spectral data of ArO aqueous solution were kinetically examined by focusing on λ_{max} values at different recorded

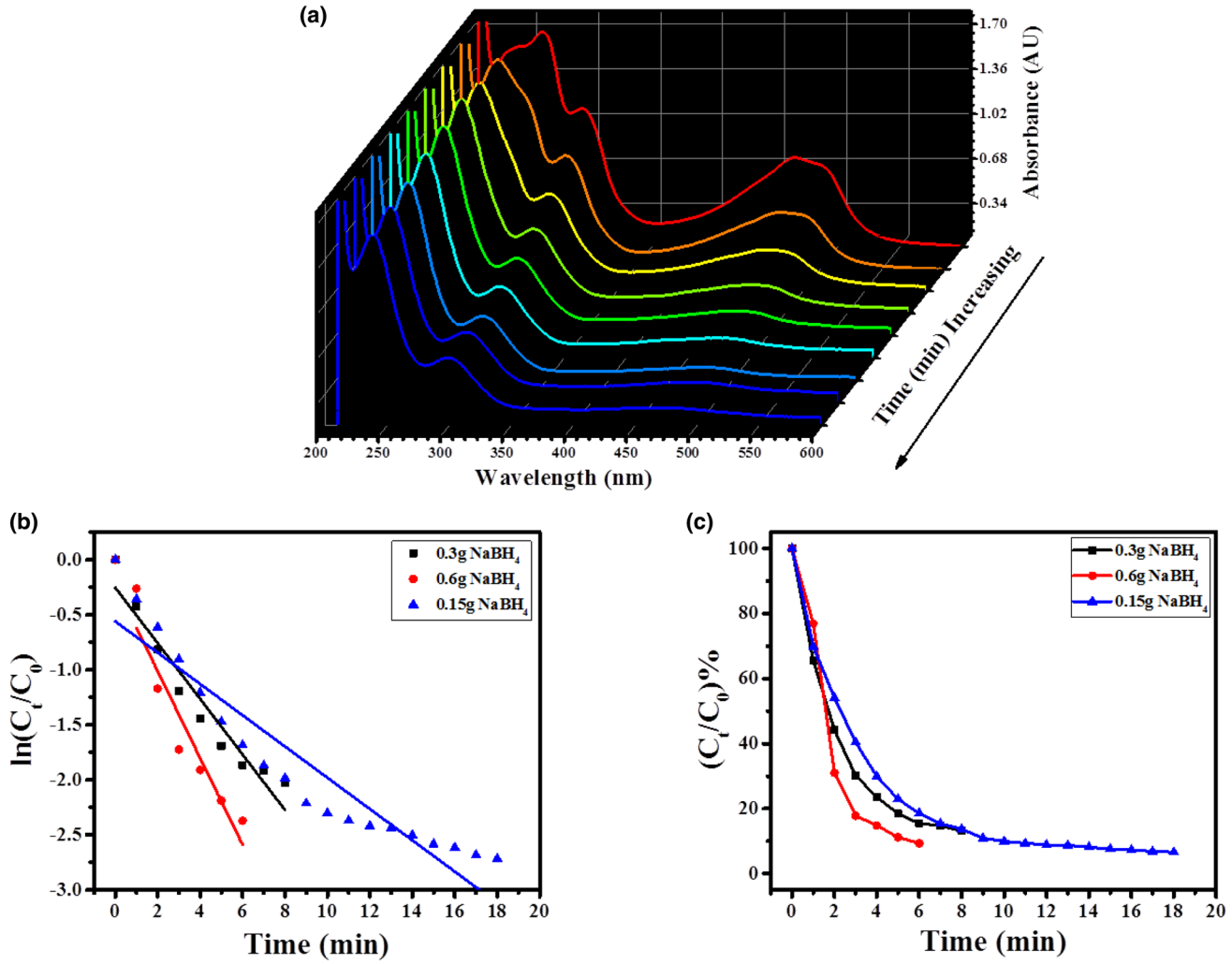

Fig. 5 Typical ArO (0.14 mM in water) reduction process by $NaBH_4$ as observed by measuring the UV-visible spectra from its aqueous solution (**a**), $\ln(C_t/C_0)$ vs time (**b**) and C_t/C_0 (%) vs time (**c**). The effect of change of the amount of $NaBH_4$ on the kinetics of the ArO reduction was studied where black cubes = 0.3 g, blue triangles = 0.15 g and red circle = 0.6 g and of $NaBH_4$. Time interval 1 min

times and processed with the *pseudo first-order* kinetic equation described above. Figure 5b indicates the $\ln(C_t/C_0)$ data versus time for the ArO reduction process. The slope of $\ln(C_t/C_0)$ versus time was used to calculate the rate of reaction. The observed reaction rate as determined from the experimental data $K_{app} = 0.253\ min^{-1}$. To further explore this reduction reaction, two more fresh reactions were performed. Other conditions were same as above except that the amount of $NaBH_4$ was changed to 0.15 g and 0.6 g using 30 ml of ArO dye solution and 0.1 g of Ag-CH. The $\ln(C_t/C_0)$ versus t data have been displayed for the above two reactions in Fig. 5b. The K_{app} values of 0.142 and 0.394 min^{-1} were noted from the Ag-CH catalyzed ArO reduction using 0.15 and 0.6 g of the reducing agent, respectively. Figure 5c reveals the residual ArO dye concentration (C_t/C_0 (%)) in the stepwise reduction reaction. According to this figure, less than 5% ArO remained after each reduction reaction, indicating that the effectiveness of the Ag-CH catalyst was high.

Based-on the results obtained in this experimental work, the following mechanism could be described. The interaction between the BH_4^{-1} and reducible species occur on the surface of the Ag nanoparticles present in the Ag-CH hydrogel. The porous hydrogel may easily allow the adsorption of the species towards the Ag nanoparticles. After the electron donation process aided by the Ag nanoparticles to the adsorbed species, a desorption of the newly formed product takes place.

To date, many catalysts have been used to catalyze these reactions and some notable studies were mentioned in the following text. Table 1 shows the catalytic performance of different catalysts previously mentioned in the literature for the reduction of 2-NP and ArO. Farhadi et al. synthesized a nanocomposite of bismuth subcarbonate–zinc ferrite

Table 1 The reduction of two organic pollutants using a sodium borohydride in the presence of different catalysts

Organic pollutant	Nanocatalyst	Time/min	Ref.
2-NP	$Bi_2O_2CO_3/ZnFe_2O_4$	17	[59]
	Ag/TP	16	[60]
	PPA_3/Fe_3O_4–Cu	25	[61]
	$Ag_3PO_4/CoFe_2O_4$	46	[62]
	Au@Fe_3O_4 yolk shell	8	[63]
	Ag-CH hydrogel	6	This work
ArO	Cu/CH-PUS	16	[43]
	Ag/Padina tetrastromatica	20	[64]
	Nanozerovalent iron (NZVI)	15	[65]
	Cu/CS–TiO_2-15	13	[66]
	Ag-CH hydrogel	6	This work

($Bi_2O_2CO_3/ZnFe_2O_4$) catalyst for the reduction of nitrophenols and nitroaniline. Their sheet-like nanocomposite catalyst was able to reduce the 2-NP in 17 min. Similarly, Ag/TP, PPA_3/Fe_3O_4–Cu, $Ag_3PO_4/CoFe_2O_4$, and Au@Fe_3O_4yolk shell catalysts reduced the 2-NP in 16, 25, 46 and 8 min, respectively. In contrast to these results, Ag-CH hydrogels swiftly reduced the 2-NP in 6 min of time. Information regarding different catalysts, used for the reduction of ArO, were gathered from the literature and presented in Table 1 for comparison with our prepared catalyst. Ag-CH hydrogels as compared to the literature reports also outperformed in the reduction of ArO.

Recycling and reuse of nanocatalysts are beneficial for the industry as it lowers the product cost. Therefore, the recycling of Ag-CH hydrogel was investigated towards the reduction of 2-NP to 2-AP in aqueous solution in presence of $NaBH_4$. After completion of the reaction, Ag-CH hydrogel catalyst was recycled simply by taking it out of the reaction media by filtering the solution and subsequently used for the next experiment. Thus, an Ag-CH catalyst was three times used in both reduction reactions. Figure 6 shows the recyclability of Ag-CH catalyst for ArO and 2-NP with respect to time. The results obtained showed that Ag-CH hydrogel shows complete reusability over three consecutive cycles with a slight loss of catalytic activity. The Ag-CH completed the reduction reactions within quite short times while the next two cycles took longer times. As shown in Fig. 6, the same catalyst was used for three reactions of ArO which took 8, 11 and 13 min to fully reduce the organic compound while in case of 2-NP it took 17, 20 and 21 min for its more than 90% reduction. A case study shows that this work exhibits higher or comparable efficiencies than other systems in terms of simple synthesis, inexpensive and nominal nanocatalysts reusability, mild reaction conditions, short reaction times and high throughput products.

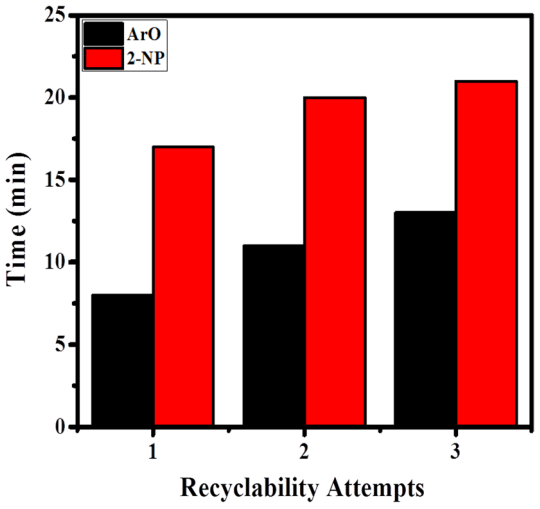

Fig. 6 Recyclability tests on the Ag-CH hydrogel catalyst during its single dose use over three time during the reduction reactions of 2-NP and ArO

Conclusion

Ag nanoparticles were successfully prepared in chitosan hydrogel matrix by a facile method of using the polymer chains as reducing agent. The Ag ions absorbed from the aqueous solution by the chitosan hydrogel were slowly transformed to Ag nanoparticles by chitosan chains. The process was validated by the color change of the Ag-CH hydrogel from clear to brown. The obtained Ag-CH samples and pure chitosan hydrogels were characterized by FESEM, XRD and EDS procedures. All these procedures successfully indicated the formation of Ag nanoparticles within chitosan hydrogels. To further apply the prepared Ag-CH, the two reduction reactions of 2-NP and ArO were chosen. Both compound aqueous solutions were reduced with $NaBH_4$ as a reducing material which the Ag-CH pieces acted as catalyst. The obtained rate constants of 0.260 and 0.253 min^{-1} were calculated for 2-NP and ArO, respectively. The catalytic Ag nanoparticles present in the chitosan hydrogel were easily retrieved and directly utilized in another one, thus proving good recyclability. Based-on the results described in this article, we predict applying this developed material as a catalyst for some other important reactions.

Acknowledgements This work was supported by the Deanship of Scientific Research (DSR), King Abdulaziz University, Jeddah, under Grant No. (D-303-130-1441). The authors, therefore, gratefully acknowledge DSR technical and financial support.

References

1. Lazar MA, Varghese S, Nair SS (2012) Photocatalytic water treatment by titanium dioxide: recent updates. Catalysts 2:572–601. https://doi.org/10.3390/catal2040572

2. Yang J, Chen C, Ji H, Ma W, Zhao J (2005) Mechanism of TiO_2-assisted photocatalytic degradation of dyes under visible irradiation: photoelectrocatalytic study by TiO_2-film electrodes. J Phys Chem B 109:21900–21907. https://doi.org/10.1021/jp0540914
3. Ansari MO, Khan MM, Ansari SA, Cho MH (2015) Polythiophene nanocomposites for photodegradation applications: past, present and future. J Saudi Chem Soc 19:494–504. https://doi.org/10.1016/j.jscs.2015.06.004
4. Bubacz K, Choina J, Dolat D, Morawski AW (2010) Methylene blue and phenol photocatalytic degradation on nanoparticles of anatase TiO_2. Polish J Environ Stud 19(4):685–691
5. Habib MA, Muslim M, Shahadat MT, Islam MN, Ismail IMI, Islam TSA, Mahmood AJ (2013) Photocatalytic decolorization of crystal violet in aqueous nano-ZnO suspension under visible light irradiation. J Nanostruct Chem 3:70
6. Rahman MM, Choudhury FA, Hossain MD, Chowdhury MNI, Mohsin S, Hasan MM, Uddin MF, Sarker NC (2012) A Comparative study on the photocatalytic degradation of industrial dyes using modified commercial and synthesized TiO_2 photocatalysts. J Chem Eng 1(27):65–71. https://doi.org/10.3329/jce.v27i2.17805
7. Rezig W, Hadjel M (2014) Photocatalytic degradation of Vat Green 03 textile dye, using the ferrihydrite-modified diatomite with TiO_2/UV process. Orient J Chem 30:993–1007
8. Vinu R, Akki SU, Madras G (2010) Investigation of dye functional group on the photocatalytic degradation of dyes by nano-TiO_2. J Hazard Mater 176:765–773. https://doi.org/10.1016/j.jhazmat.2009.11.101
9. Kamal T, Khan SB, Asiri AM (2016) Synthesis of zero-valent Cu nanoparticles in the chitosan coating layer on cellulose microfibers: evaluation of azo dyes catalytic reduction. Cellulose 23:1911–1923. https://doi.org/10.1007/s10570-016-0919-9
10. Kamal T, Anwar Y, Khan SB, Chani MTS, Asiri AM (2016) Dye adsorption and bactericidal properties of TiO_2/chitosan coating layer. Carbohydr Polym 148:153–160. https://doi.org/10.1016/j.carbpol.2016.04.042
11. Kamal T, Ahmad I, Khan SB, Asiri AM (2017) Synthesis and catalytic properties of silver nanoparticles supported on porous cellulose acetate sheets and wet-spun fibers. Carbohydr Polym 157:294–302. https://doi.org/10.1016/j.carbpol.2016.09.078
12. Ahmad I, Kamal T, Khan SB, Asiri AM (2016) An efficient and easily retrievable dip catalyst based on silver nanoparticles/chitosan-coated cellulose filter paper. Cellulose 23:3577–3588. https://doi.org/10.1007/s10570-016-1053-4
13. Ahmad I, Khan SB, Kamal T, Asiri AM (2017) Visible light activated degradation of organic pollutants using zinc–iron selenide. J Mol Liq 229:429–435. https://doi.org/10.1016/j.molliq.2016.12.061
14. Ali N, Ismail M, Khan A, Khan H, Haider S, Kamal T (2018) Spectrophotometric methods for the determination of urea in real samples using silver nanoparticles by standard addition and 2nd order derivative methods. Spectroc Biomol Acta Pt A 189:110–115. https://doi.org/10.1016/j.saa.2017.07.063
15. Ali F, Khan SB, Kamal T, Anwar Y, Alamry KA, Asiri AM (2017) Bactericidal and catalytic performance of green nanocomposite based on chitosan/carbon black fiber supported monometallic and bimetallic nanoparticles. Chemosphere 188:588–598. https://doi.org/10.1016/j.chemosphere.2017.08.118
16. Ali N, Awais T, Kamal M, Ul-Islam A, Khan SJ, Shah A, Zada (2018) Chitosan-coated cotton cloth supported copper nanoparticles for toxic dye reduction. Int J Biol Macromol 111:832–838. https://doi.org/10.1016/j.ijbiomac.2018.01.092
17. Ali F, Khan SB, Kamal T, Alamry KA, Asiri AM, Sobahi TRA (2017) Chitosan coated cotton cloth supported zero-valent nanoparticles: simple but economically viable, efficient and easily retrievable catalysts. Sci Rep 7:16957. https://doi.org/10.1038/s41598-017-16815-2
18. Dodoo-Arhin D, Buabeng FP, Mwabora JM, Amaniampong PN, Agbe H, Nyankson E, Obada DO, Asiedu NY (2018) The effect of titanium dioxide synthesis technique and its photocatalytic degradation of organic dye pollutants. Heliyon 4:e00681. https://doi.org/10.1016/j.heliyon.2018.e00681
19. Lanka SS (2015) Methods of removing heavy metals from industrial wastewater. J Multidiscip Eng Sci Stud 1:14
20. Krstić V, Urošević T, Pešovski B (2018) A review on adsorbents for treatment of water and wastewaters containing copper ions. Chem Eng Sci 192:273–287. https://doi.org/10.1016/j.ces.2018.07.022
21. Ahmed E, Nagaoka K, Fayez M, Abdel-Daim MM, Samir H, Watanabe G (2015) Suppressive effects of long-term exposure to *P*-nitrophenol on gonadal development, hormonal profile with disruption of tissue integrity, and activation of caspase-3 in male Japanese quail (Coturnix japonica). Environ Sci Pollut Res 22:10930–10942. https://doi.org/10.1007/s11356-015-4245-9
22. Ahmed E, Nagaoka K, Fayez M, Samir H, Watanabe G (2015) Long-term p-nitrophenol exposure can disturb liver metabolic cytochrome P450 genes together with aryl hydrocarbon receptor in Japanese quail. Jpn J Vet Res 63:115–127. https://doi.org/10.14943/jjvr.63.3.115
23. Bae S, Gim S, Kim H, Hanna K (2016) Effect of $NaBH_4$ on properties of nanoscale zero-valent iron and its catalytic activity for reduction of *p*-nitrophenol. Appl Catal B 182:541–549. https://doi.org/10.1016/j.apcatb.2015.10.006
24. Bilici A, Ayten B, Kaya İ (2015) Facile preparation of gold nanoparticles on the polyquinoline matrix: catalytic performance toward 4-nitrophenol reduction. Synth Met 201:11–17. https://doi.org/10.1016/j.synthmet.2015.01.009
25. Gao J, Xu J, Wen S, Hu J, Liu H (2015) Plasma-assisted synthesis of Ag nanoparticles immobilized in mesoporous cellular foams and their catalytic properties for 4-nitrophenol reduction. Microporous Mesoporous Mater 207:149–155. https://doi.org/10.1016/j.micromeso.2015.01.025
26. Kamal T, Ahmad I, Khan SB, Asiri AM (2019) Anionic polysaccharide stabilized nickel nanoparticles-coated bacterial cellulose as a highly efficient dip-catalyst for pollutants reduction. React Funct Polym 145:104395. https://doi.org/10.1016/j.reactfunctpolym.2019.104395
27. Kamal T, Ahmad I, Khan SB, Ul-Islam M, Asiri AM (2019) Microwave assisted synthesis and carboxymethyl cellulose stabilized copper nanoparticles on bacterial cellulose nanofibers support for pollutants degradation. J Polym Environ 27:2867–2877. https://doi.org/10.1007/s10924-019-01565-1
28. Kamal T, Ali N, Naseem AA, Khan SB, Asiri AM (2016) Polymer nanocomposite membranes for antifouling nanofiltration. Recent Pat Nanotechnol 10:189–201. https://doi.org/10.2174/1872210510666160429145704
29. Zaman A, Ahmad I, Pervaiz M, Ahmad S, Kiran S, Khan MA, Gulzar T, Kamal T (2019) A novel synthetic approach for the synthesis of pyrano[3,2-c] quinolone-3carbaldehydes by using modified Vilsmeier Haack reaction, as potent antimicrobial agents. J Mol Struct 1180:227–236. https://doi.org/10.1016/j.molstruc.2018.11.030
30. Abdelghany AM, Mekhail MSh, Abdelrazek EM, Aboud MM (2015) Combined DFT/FTIR structural studies of monodispersed PVP/gold and silver nano particles. J Alloys Compd 646:326–332. https://doi.org/10.1016/j.jallcom.2015.05.262
31. Palaniappan P, Sathishkumar G, Sankar R (2015) Fabrication of nano-silver particles using Cymodocea serrulata and its cytotoxicity effect against human lung cancer A549 cells line. Spectrochim Acta A 138:885–890. https://doi.org/10.1016/j.saa.2014.10.072

32. Ahmad I, Kamal T, Khan SB, Asiri AM (2016) An efficient and easily retrievable dip catalyst based on silver nanoparticles/chitosan-coated cellulose filter paper. Cellulose. 23:3577–3588. https://doi.org/10.1007/s10570-016-1053-4
33. Kamal T, Khan SB, Haider S, Alghamdi YG, Asiri AM (2017) Thin layer chitosan-coated cellulose filter paper as substrate for immobilization of catalytic cobalt nanoparticles. Int J Biol Macromol 104:56–62. https://doi.org/10.1016/j.ijbiomac.2017.05.157
34. Kamal T, Khan SB, Asiri AM (2016) Nickel nanoparticles-chitosan composite coated cellulose filter paper: an efficient and easily recoverable dip-catalyst for pollutants degradation. Environ Pollut 218:625–633. https://doi.org/10.1016/j.envpol.2016.07.046
35. Chen M, Kang H, Gong Y, Guo J, Zhang H, Liu R (2015) Bacterial cellulose supported gold nanoparticles with excellent catalytic properties. ACS Appl Mater Interfaces 7:21717–21726. https://doi.org/10.1021/acsami.5b07150
36. Kamal T, Ahmad I, Khan SB, Asiri AM (2019) Bacterial cellulose as support for biopolymer stabilized catalytic cobalt nanoparticles. Int J Biol Macromol 135:1162–1170. https://doi.org/10.1016/j.ijbiomac.2019.05.057
37. Ali F, Khan SB, Kamal T, Anwar Y, Alamry KA, Asiri AM (2017) Anti-bacterial chitosan/zinc phthalocyanine fibers supported metallic and bimetallic nanoparticles for the removal of organic pollutants. Carbohydr Polym 173:676–689. https://doi.org/10.1016/j.carbpol.2017.05.074
38. Kamal T, Ahmad I, Khan SB, Asiri AM (2017) Synthesis and catalytic properties of silver nanoparticles supported on porous cellulose acetate sheets and wet-spun fibers. Carbohydr Polym 157:294–302. https://doi.org/10.1016/j.carbpol.2016.09.078
39. Ahmed MS, Kamal T, Khan SA, Anwar Y, Saeed MT, Asiri AM, Khan SB (2016) Assessment of anti-bacterial Ni-Al/chitosan composite spheres for adsorption assisted photo-degradation of organic pollutants. Curr Nanosci 12:569–575. https://doi.org/10.2174/1573413712666160204000517
40. Khan SB, Ali F, Kamal T, Anwar Y, Asiri AM, Seo J (2016) CuO embedded chitosan spheres as antibacterial adsorbent for dyes. Int J Biol Macromol 88:113–119. https://doi.org/10.1016/j.ijbiomac.2016.03.026
41. Khan SB, Khan SA, Marwani HM, Bakhsh EM, Anwar Y, Kamal T, Asiri AM, Akhtar K (2016) Anti-bacterial PES-cellulose composite spheres: dual character toward extraction and catalytic reduction of nitrophenol. RSC Adv 6:110077–110090. https://doi.org/10.1039/c6ra21626a
42. Khan MSJ, Khan SB, Kamal T, Asiri AM (2019) Agarose biopolymer coating on polyurethane sponge as host for catalytic silver metal nanoparticles. Polym Test 78:105983. https://doi.org/10.1016/j.polymertesting.2019.105983
43. Khan MSJ, Kamal T, Ali F, Asiri AM, Khan SB (2019) Chitosan-coated polyurethane sponge supported metal nanoparticles for catalytic reduction of organic pollutants. Int J Biol Macromol 132:772–783. https://doi.org/10.1016/j.ijbiomac.2019.03.205
44. Alshehri SM, Almuqati T, Almuqati N, Al-Farraj E, Alhokbany N, Ahamad T (2016) Chitosan based polymer matrix with silver nanoparticles decorated multiwalled carbon nanotubes for catalytic reduction of 4-nitrophenol. Carbohydr Polym 151:135–143. https://doi.org/10.1016/j.carbpol.2016.05.018
45. Rahman MM, Wahid A, Alam MM, Asiri AM (2018) Efficient 4-nitrophenol sensor development based on facile Ag@Nd_2O_3 nanoparticles. Mater Today Commun 16:307–313. https://doi.org/10.1016/j.mtcomm.2018.07.009
46. Lee CH, Singla A, Lee Y (2001) Biomedical applications of collagen. Int J Pharm 221:1–22. https://doi.org/10.1016/S0378-5173(01)00691-3
47. Lee KY, Mooney DJ (2001) Hydrogels for tissue engineering. Chem Rev 101:1869–1880. https://doi.org/10.1021/cr000108x
48. Haider S, Kamal T, Khan SB, Omer M, Haider A, Khan FU, Asiri AM (2016) Natural polymers supported copper nanoparticles for pollutants degradation. Appl Surf Sci 387:1154–1161. https://doi.org/10.1016/j.apsusc.2016.06.133
49. Ajmal M, Demirci S, Siddiq M, Aktas N, Sahiner N (2016) Simultaneous catalytic degradation/reduction of multiple organic compounds by modifiable *p*(methacrylic acid-*co*-acrylonitrile)-M (M: Cu, Co) microgel catalyst composites. New J Chem 40:1485–1496. https://doi.org/10.1039/c5nj02298c
50. Farooqi ZH, Tariq N, Begum R, Khan SR, Iqbal Z, Khan A (2015) Fabrication of silver nanoparticles in poly(*N*-isopropylacrylamide-*co*-allylacetic acid) microgels for catalytic reduction of nitroarenes. Turk J Chem 39:576–588. https://doi.org/10.3906/kim-1412-15
51. ur Rehman S, Siddiq M, Al-Lohedan H, Sahiner N (2015) Cationic microgels embedding metal nanoparticles in the reduction of dyes and nitro-phenols. Chem Eng J 265:201–209. https://doi.org/10.1016/j.cej.2014.12.061
52. Sahiner N, Ozay H, Ozay O, Aktas N (2010) A soft hydrogel reactor for cobalt nanoparticle preparation and use in the reduction of nitrophenols. Appl Catal B 101:137–143. https://doi.org/10.1016/j.apcatb.2010.09.022
53. Rocha-García D, Betancourt-Mendiola MdeL, Wong-Arce A, Rosales-Mendoza S, Reyes-Hernández J, González-Ortega O, Palestino G (2018) Gelatin-based porous silicon hydrogel composites for the controlled release of tramadol. Eur Polym J 108:485–497. https://doi.org/10.1016/j.eurpolymj.2018.09.033
54. Ghosh SK, Das A, Basu A, Halder A, Das S, Basu S, Abdullah MdF, Mukherjee A, Kundu S (2018) Semi-interpenetrating hydrogels from carboxymethyl guar gum and gelatin for ciprofloxacin sustained release. Int J Biol Macromol 120:1823–1833. https://doi.org/10.1016/j.ijbiomac.2018.09.212
55. Ghosh SK, Mandal M, Kundu S, Nath S, Pal T (2004) Bimetallic Pt–Ni nanoparticles can catalyze reduction of aromatic nitro compounds by sodium borohydride in aqueous solution. Appl Catal A 268:61–66. https://doi.org/10.1016/j.apcata.2004.03.017
56. Kamal T (2019) Aminophenols formation from nitrophenols using agar biopolymer hydrogel supported CuO nanoparticles catalyst. Polym Test 77:105896. https://doi.org/10.1016/j.polymertesting.2019.105896
57. Shi X, Quan S, Yang L, Shi G, Shi F (2019) Facile synthesis of magnetic Co_3O_4/BFO nanocomposite for effective reduction of nitrophenol isomers. Chemosphere 219:914–922. https://doi.org/10.1016/j.chemosphere.2018.12.045
58. Kamal T, Ahmad I, Khan SB, Asiri AM (2018) Agar hydrogel supported metal nanoparticles catalyst for pollutants degradation in water. Desalin Water Treat 136:290–298. https://doi.org/10.5004/dwt.2018.23230
59. Zarringhadam P, Farhadi S (2018) Novel sheet-like bismuth subcarbonate-zinc ferrite ($Bi_2O_2CO_3$/$ZnFe_2O_4$) magnetically recyclable nanocomposites: synthesis, characterization and enhanced catalytic performance for the reduction of nitrophenols and nitroanilines. Appl Organomet Chem 32:e4518. https://doi.org/10.1002/aoc.4518
60. Ismail M, Khan MI, Khan SB, Akhtar K, Khan MA, Asiri AM (2018) Catalytic reduction of picric acid, nitrophenols and organic azo dyes via green synthesized plant supported Ag nanoparticles. J Mol Liq 268:87–101. https://doi.org/10.1016/j.molliq.2018.07.030
61. Abou El FI, Fadl GA, Mahmoud AA, Mohamed (2019) Effect of metal nanoparticles on the catalytic activity of pectin(poly vinyl alcohol-co-polyacrylamide) nanocomposite hydrogels. J Inorg Organomet Polym 29:332–339. https://doi.org/10.1007/s10904-018-1003-8
62. Abroushan E, Farhadi S, Zabardasti A (2017) Ag_3PO_4 /$CoFe_2O_4$ magnetic nanocomposite: synthesis, characterization and

applications in catalytic reduction of nitrophenols and sunlight-assisted photocatalytic degradation of organic dye pollutants. RSC Adv 7:18293–18304. https://doi.org/10.1039/C7RA01728F

63. Lin F, Doong R (2017) Catalytic nanoreactors of Au@Fe_3O_4 yolk–shell nanostructures with various Au sizes for efficient nitroarene reduction. J Phys Chem C 121:7844–7853. https://doi.org/10.1021/acs.jpcc.7b00130
64. Barnabas CGS, Santhanam A (2018) Comparative photocatalytic degradation of organic dyes using silver nanoparticles synthesized from padina tetrastromatica. Curr Nanosci. http://www.eurekaselect.com/155164/article. Accessed 1 Jul 2019
65. Prema P, Thangapandian S, Selvarani M, Subharanjani S, Amutha C (2011) Color removal efficiency of dyes using nanozerovalent iron treatment. Toxicol Environ Chem 93:1908–1917. https://doi.org/10.1080/02772248.2011.606613
66. Ali F, Khan SB, Kamal T, Alamry KA, Asiri AM (2018) Chitosan-titanium oxide fibers supported zero-valent nanoparticles: highly efficient and easily retrievable catalyst for the removal of organic pollutants. Sci Rep 8:6260. https://doi.org/10.1038/s41598-018-24311-4

Publisher's Note Springer Nature remains neutral with regard to jurisdictional claims in published maps and institutional affiliations.